



HAL
open science

Assessment of leaching risk of trace metals, PAHs and PCBs from a brownfield located in a flooding zone

Martin Seidl, Julien Le Roux, Rémi Mazerolles, Nouredine Bousserrhine

► To cite this version:

Martin Seidl, Julien Le Roux, Rémi Mazerolles, Nouredine Bousserrhine. Assessment of leaching risk of trace metals, PAHs and PCBs from a brownfield located in a flooding zone. Environmental Science and Pollution Research, inPress, 10.1007/s11356-021-15491-0 . hal-03321258

HAL Id: hal-03321258

<https://enpc.hal.science/hal-03321258>

Submitted on 17 Aug 2021

HAL is a multi-disciplinary open access archive for the deposit and dissemination of scientific research documents, whether they are published or not. The documents may come from teaching and research institutions in France or abroad, or from public or private research centers.

L'archive ouverte pluridisciplinaire **HAL**, est destinée au dépôt et à la diffusion de documents scientifiques de niveau recherche, publiés ou non, émanant des établissements d'enseignement et de recherche français ou étrangers, des laboratoires publics ou privés.

Assessment of leaching risk of trace metals, PAHs and PCBs from a brownfield located in a flooding zone

Martin SEIDL^{1*}, Julien LE ROUX², Rémi MAZEROLLES¹, Nouredine BOUSSERRHINE²

¹LEESU ENPC, Université Paris-Est, 6-8 avenue Blaise Pascal, 77455, cedex 2 Marne la Vallée, France

²LEESU UPEC, Université Paris-Est Créteil, 61 avenue du Général de Gaulle, 94010 Créteil Cedex, France

* Corresponding author: martin.seidl@enpc.fr

Abstract

An old industrial site (brownfield) located south of Paris in a flooding plain and containing demolition disposal as well as a burning zone for metal recovery is being regenerated to satisfy local need for public green space. The main objective of the described study was therefore to assess the risk of remobilisation of trace metals, PAH and PCB present. The research focused on vertical migration due to rainfall (non-saturated flow) and to river flooding (saturated flow). To assess the remobilisation risk, representative soil profiles were reconstituted and eluted in columns with artificial rain and filtered river water for six weeks with an equivalent of 25 mm d⁻¹. Soil analysis showed that both zones are highly contaminated, exceeding the French environmental standards. Though the superficial metal content was much higher in the burning zone with levels of g kg⁻¹ than in the demolition zone, most metals showed higher levels in the eluents of the latter. The level of dissolved Zn in the burning-zone eluent was 30 µg L⁻¹ while in the demolition-zone it was 300 µg L⁻¹, 40 times the admissible level. Zn was thereby correlated to aromaticity parameter HIX, indicating a link with organic matter transformation. The Cu was only significantly released under saturated condition (up to 80 µg L⁻¹) in the demolition soil, indicating as implicated mechanism manganese and iron oxide reduction rather than organic matter transformation. Despite the high PAH and PCB soil contents, these pollutants were not released. The total PAH content in the effluent was 30 ng L⁻¹ in average and did not significantly differ between the two zones and the types of hydrology. Only Zn and Cu issued from demolition zone presented an eco-toxicological risk. Crossed statistical analysis of the results showed that the role of the soil type is preponderant in the pollutant release and that temporary flooding condition would induce a lower impact on the ground water quality than an equivalent amount of fallen rain. Though the burning site was far more contaminated in the upper soil than the demolition zone, it presented little risk compared to the demolition-zone, more profound and more permeable. The latter showed therefore significative trace metal release, up to 2.1 kg ha⁻¹ year⁻¹ for zinc, doubling the local atmospheric deposition.

Keywords

Soil contamination; Pollutant remobilisation; Rain; Flood; Heavy metals; Organic micropollutants; Saturated and unsaturated flow conditions; Column experiments; Environmental impact

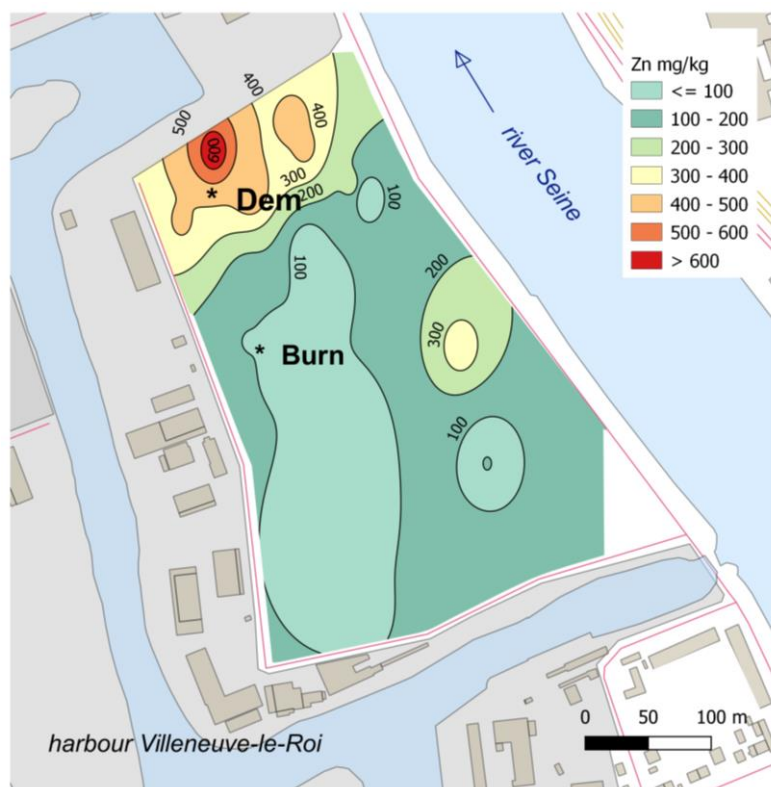
Introduction

Generally, brownfield sites exist in a city's or town's industrial sections, on locations with abandoned factories or commercial buildings or other previously polluting activities. Typical contaminants found on contaminated brownfield land include hydrocarbon spillages, solvents and heavy metals. The regeneration of brownfields has gained prominence due to their potential to satisfy urban expansion and to promote green areas.

48 In France, the most treated pollutants in brownfield soils are the total hydrocarbons (HC), the
49 organohalogen volatile compounds (OHVC) and heavy metals, representing together nearly 80% of
50 the brownfield pollutants. The principal pollutants in groundwaters are also OHVC and HC,
51 representing 47% of the pollutants. The “other pollutants” usually include cyclohexane,
52 pentachlorophenol (PCP), asbestos, cyanides and sulphates (ADEME 2014).

53
54 The Pierre-Fitte study site (ENPF 2017) is located in the industrial area of Villeneuve-le-Roi (France),
55 more particularly in the docks of Carelle port on the left bank of the river Seine, 20 km upstream of
56 Paris. It is representative of typical polluted brownfields, with high levels of heavy metals and several
57 spots of organic micropollutants (Guittard *et al.* 2013). The long-term annual precipitation of the
58 region is 650 mm, and the mean annual air temperature is 12.1 °C. The area still accommodates various
59 types of companies like trade of construction material, recycling of paper and scrap and petrol deposit
60 (Souvestre 2013). The site may be periodically flooded in the spring by the river Seine depending on
61 rain distribution and dam management upstream (DRIEE 2015). The flood return period is about 25
62 years, and the last ones registered occurred in 2016 and 2018 (DRIEE 2018). Since the 3-ha brownfield
63 is planned to be regenerated as green space for local inhabitants, local authorities evaluated its sanitary
64 risks in 2013 (Guittard and *et al.* 2013). The area shows two main zones of contamination: a 50-year-
65 old demolition disposal (called DEM) and a more recent spot where electric equipment was burned
66 for metal recovery (called BURN) (Figure 1). The heavy metal content of the DEM zone is actually
67 too high to allow public access and should be therefore decontaminated in the future by
68 phytoremediation. The Zn concentration map based on the data obtained from the preliminary risk
69 assessment (Guittard and *et al.* 2013) is shown in Figure 1.

70



71

72

73 **Fig. 1** Position of the brownfield and the sampling sites DEM and BURN, together with the intensity
74 of zinc contamination (ppm), using the data of CD94 County survey (Guittard *et al.* 2013). The bottom
75 left corner corresponds to GPS coordinates 48.7374427 N, 2.4371572 E.

76

77 Floodplains act as a link between terrestrial and aquatic ecosystems. They underlie large seasonal
78 fluctuations of the water table that induce varying compositions of the interstitial solution and redox
79 conditions. Moreover, periodical floods result in the deposition of sediments and casually in
80 concomitant inputs of dissolved and particulate contaminants. Varying conditions of redox potential,
81 which are seasonally found in floodplain soils (Shaheen and Rinklebe 2014), may induce the
82 precipitation or reductive bacterial dissolution of Mn and Fe oxides acting as carrier phases for heavy
83 metals and, under strictly reducing conditions, the formation of sparingly soluble metal sulphides
84 (Bousserrhine et al. 1999; Suna Erses and Onay 2003; Du Laing et al. 2009; Gounou et al. 2010;
85 Harris-Hellal et al. 2011). Even though the river Seine floods upstream of Paris are relatively short
86 events (level rise during 1 or 2 days, level decrease 1 or 2 weeks), such conditions might also be
87 present in the area studied.

88
89 On most contaminated sites, monitoring of groundwater and interstitial water is not feasible due to
90 field conditions like lack of physical accessibility, high heterogeneity of underground, administrative
91 limitations and limited financial support. Therefore, laboratory tests have been set up to simulate field
92 conditions and to allow sampling of all components using simplified techniques (Van der Sloot 1996).
93 Numerous procedures exist to simulate the leaching of pollutants from soil (Dermont et al. 2008; US
94 EPA 2015). These tests can be principally divided in batch-leaching tests (i.e. a soil sample is leached
95 with water or a specific solution at a predefined liquid/solid (L/S) ratio and reaction time) and column
96 experiments, where contaminant release from soil is studied under controlled and more realistic flow
97 conditions. Column experiments offer, moreover, the option of modification of experimental
98 conditions like flow velocities and flow interruptions to better identify the kinetics of contaminant
99 release (Rennert et al. 2010). To estimate the metal mobility, numerous studies determined the
100 sequential metal content (Thums et al. 2008; Gounou et al. 2010; Li et al. 2015) or standardised
101 leachability of organic pollutants (Van der Sloot 1996; Reemtsma and Mehrtens 1997; Cappuyns and
102 Swennen 2008; Tian et al. 2015; US EPA 2017; ISO 2019), but only few of them focused on
103 biogeochemical or hydrological process involved in pollutant release and behaviour (Gounou et
104 al.2010; Harris et al. 2011; Fang et al. 2016). Although natural leaching processes occurring in situ
105 can be best reproduced in the laboratory by column experiments with undisturbed soil or sediment
106 profile (Camobreco et al. 1996; Schuwirth and Hofmann 2006), only few recent papers use this
107 approach, principally due to a more complex and work-intensive methodology (Pot et al. 2011;
108 Gonzalez et al. 2019; Cueff et al. 2020). Nevertheless, these authors use simplified, constant and
109 unsaturated flow conditions. Some authors, like Rennert and Rinklebe (2010), used a saturated
110 approach to compensate these shortcomings, though they applied homogenised sieved soils. The
111 originality of our paper is therefore a combination of column experiments with reconstituted natural
112 soil profiles and intermittent, saturated and unsaturated flows to assess the mobilisation risk as close
113 as possible to the hydrological field conditions.

114
115 Based on a preliminary environmental assessment (Guittard and et al. 2013) revealing contamination
116 with heavy metals, the main objective of this study was to provide an extensive evaluation of in-depth
117 contamination by trace metals, PAH and PCB and to evaluate their mobility according to various
118 hydrological scenarios present on site. The aim of proposed work was therefore to answer the
119 following specific questions: What is the risk of contamination of groundwater linked to present
120 contamination? Is there any specific risk of remobilisation of pollutants due to flooding? To what
121 degree do the soil structure and biogeochemical conditions contribute to the pollutant mobility? What
122 are the differences between trace metals and organic micropollutants in terms of remobilisation and
123 associated processes?

124
125
126

127 **Materials and methods**

128

129 As the process in situ is more accurately simulated by column experiments (Schuwirth and Hofmann
130 2006), with undisturbed soil profile (Camobreco et al. 1996), this approach was applied in the present
131 study. Due to the presence of large fragments of construction material or electric cables in the soil, it
132 was not possible to get undisturbed soil columns in situ and reconstitution of representative soil
133 profiles was performed in the laboratory. Since the brownfield is situated in the flooding zone, the
134 evaluation focused on the (vertical) pollutant mobility induced by rainfall (non-saturated percolation)
135 or as consequence of river flooding (saturated percolation). As rain and flooding are recurrent
136 processes intermittent water supply was applied.

137

138 **Soil sampling**

139 Soil sampling was carried out on two areas of the Carelle site: the DEM area, a 50-year-old demolition
140 disposal and the BURN area, a more recent spot where electric equipment was burned for metal
141 recovery, in the beginning of April 2016, 1 week after a rainfall. For each sampling area, three points
142 were chosen at equidistance (30 m for DEM and 5 m for BURN), south, east and west from the
143 pollution spot centre. At each point, surface plants and objects larger than 10 cm were removed and
144 the soil was excavated on a square of 50 by 50 cm, per layer of 10 cm to a depth of 50 cm, sufficient
145 to sample the whole organic soil horizon, the most microbiologically active layer. The soil of each
146 layer was homogenised and quartered, where after the half of one portion was taken as a representative
147 sample of the layer. In the laboratory, the soil samples were sieved at field humidity subsequently
148 with 1-cm and 2-mm mesh. The fraction of 2 mm was kept refrigerated at 6°C until the column
149 experiments and soil analysis.

150

151 **Column operation**

152 For the two sampling areas (DEM and BURN), the layers coming from the same depth of three
153 sampling points were mixed to obtain composite layers, representative for the entire area (i.e. 5
154 composite layers for each sampling area). These composite samples were used for extended soil
155 analysis and to pack the columns.

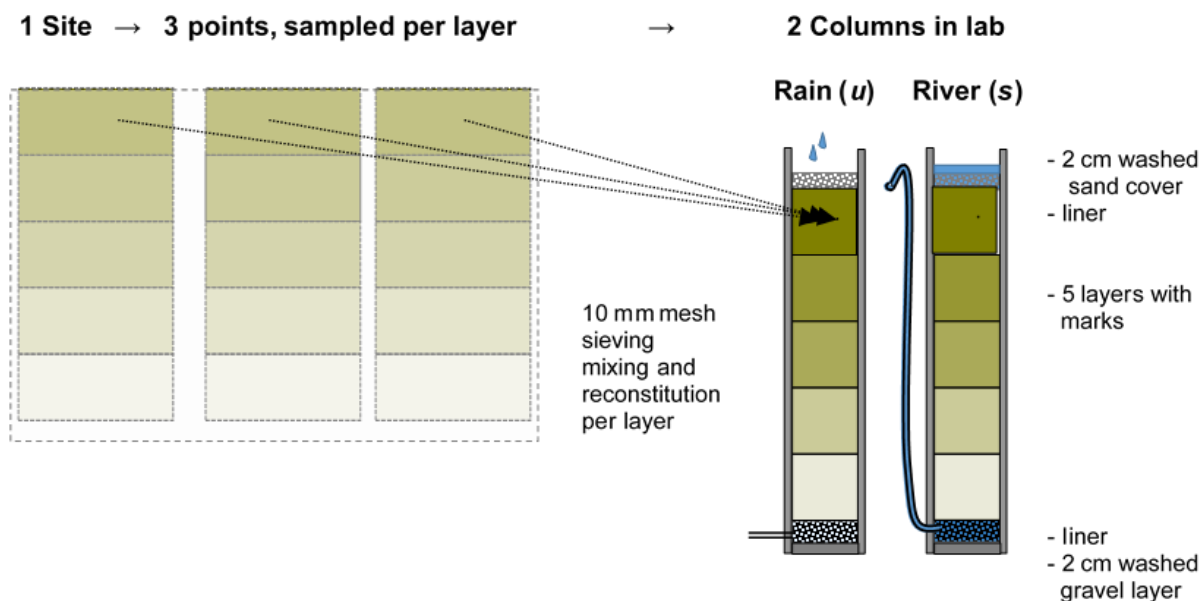
156

157 The columns were constituted from standard PVC water pipes and closures, with a large internal
158 diameter of 153 mm to avoid border effects. A drainage layer of 3 cm of gravel (mainly quartz) was
159 placed at the bottom of the column, surmounted by a PE geotextile membrane (Onduline). Gravel and
160 sand were soaked overnight in 2% nitric acid to remove any trace of limestone and metals and were
161 washed prior to use. All columns were cleaned with detergent (Extran), 2% HNO₃ and distilled water
162 before experimentation. The cleaned empty columns, together with gravel, sand and geotextile were
163 entirely filled with the same eluent used for the experiments (see below) and left for 24 h in the dark
164 at room temperature to determine the background pollution (blank samples). Afterwards, the columns
165 were packed with subsequent composite layers according to their field depth and mass, based on the
166 field wet density to constitute a representative soil profile with approximate field hydraulic
167 conductivity. The separation between layers were marked by a small stripe of geotextile to make their
168 final analysis possible. The top of the column was covered again by geotextile and a 2-cm layer of
169 quartz sand to guarantee a homogenous water distribution (Figure 2).

170

171 For each study area, DEM and BURN, two columns were prepared, one to simulate rainfall
172 (unsaturated percolation) and the other to simulate exposition during flooding (saturated elution).
173 Artificial rainwater was produced according to the rain composition in Paris region (Kafi et al. 2008;
174 Seidl et al. 2013) by diluting twice the commercial mineral water *Mont Roucoux* with MilliQ water,
175 stocked in the dark prior to use. River water came from the entrance of the harbour Villeneuve-le-Roi

176 and was filtered on oven cleaned (2h 550°C) glass microfibre filter (Whatman GF/F, approx. porosity
177 0.7 µm) and stocked in the dark prior to use.
178



179
180 **Fig. 2** Set-up and operation of unsaturated (u-DEM and u-BURN) and saturated columns (s-DEM and
181 s-BURN)
182

183 Rainfall was simulated by sprinkling 2.3 L of artificial rainwater through 5 irrigation gutters at the top
184 of the column twice a week (Monday and Thursday afternoon) at approximate flow of 1 L h^{-1} ,
185 equivalent to a “rainfall” of 125 mm (u-DEM and u-BURN) columns. Columns s-DEM and s-BURN,
186 simulating the flood conditions (fast rise of groundwater level in the beginning of the flood, followed
187 by slow infiltration of remaining flood water) were initially saturated by river water by the bottom of
188 the column, where after 2.3 L of river water was applied at the top of the column, the columns were
189 kept saturated by a siphenoid outflow. The resulting hydraulic regime corresponded to 4-6 h of
190 percolation followed by 3 days of retention. The apparent vertical Darcy velocity, determined from
191 flow and cross section, varied according to the soil type from 2 to $8 \times 10^{-5} \text{ m s}^{-1}$, similar to those found
192 in situ (Table 1) and to those used by others, in comparable set-up (Rennert et al. 2010). Whole
193 samples were collected at the bottom of the column at the end of percolation the morning after the
194 application. The total water height applied on each column was 1500 mm for 6 weeks of experiment.
195

196 Analytical methods

197 All analyses were performed following the US (APHA et al. 2012) and French (AFNOR 2002, 2005)
198 analytical and GLP recommendations. For metal analysis, certified reference materials were used for
199 result verification.
200

201 Estimation of granulometry was obtained on AFNOR-certified stainless-steel sieves at 10 mm and at
202 2 mm. All specific soil analyses were done on the crushed 2-mm fraction dried at 40°C for 7 days to
203 limit the organic pollutant evaporation/degradation. The soil humidity and porosity were estimated as
204 water loss at 105°C on unsaturated and saturated standard ring samples (100 ml) taken in each column
205 layer at the end of experiments. The soil organic matter was estimated as dry volatile matter after
206 ignition loss at 550°C for 8 h. The total organic and inorganic soil carbon content were determined on
207 COT metre (OI Analytical), and the total soil heavy metal content was screened by fluorescence X
208 (portable XRF analyser Bruker). The hydraulic conductivity was measured in the field by the Guelph
209 permeameter (Nasri et al. 2015) and determined in the laboratory as flow rate during the first hour of
210 the percolation.

211 The leachate conductivity and pH were measured using a TetraCon 325 sensor and Sentix 41-3 KCl-
212 electrode (WTW Multi-parameter 340i). Turbidity was determined with a portable turbidimeter (Hach
213 2100P).

214

215 Liquid samples for metal analysis were vacuum filtered using disposable PE tubes including 0.45- μ m
216 PTFE filters (Digiprep SA, France) and acidified by adding 1% of concentrated HNO₃ (Merck
217 ultrapure). Liquid samples for DOC and organic micropollutants analysis were vacuum filtrated on
218 oven treated (2h at 550°C) using glass support and microfibre filter (Whatman GF/F). Any vessel used
219 for the metal analysis was soaked overnight in 2% Extran detergent (Merck) aqueous solution,
220 followed by 24 h in 2% HNO₃ solution and rinsed with tap, distilled and ultra-pure water (18M Ω ,
221 MilliQ Millipore). Any vessel used for the organic micropollutant and DOC analysis was soaked
222 overnight in 2% TFD4 detergent (Franklab SA, France) aqueous solution and rinsed abundantly with
223 tap and distilled water and air-dried and, if necessary, oven cleaned at 550°C for 2 h.

224

225 Dissolved organic carbon (DOC) was measured using an IR spectrometer (OI Analytical) on filtered
226 samples preserved with 1% orthophosphoric acid (VWR, 85 %). UV absorbance was obtained on
227 filtered samples on a UV spectrometer (Secoman UV-Line 9400, France) and three-dimensional
228 fluorescence excitation-emission matrices (EEMs) were obtained on a fluorescence spectrometer
229 (Jasco FP-8300, Japan). Specific UV absorbance at 254 nm (SUVA) was calculated as the ratio
230 between UV absorbance at 254 nm and DOC concentration. Specific fluorescence indexes for
231 dissolved organic matter, BIX and HIX, were determined according to Huguet (Huguet et al. 2010)
232 and Zsolnay (Zsolnay et al. 1999).

233

234 Trace metals were analysed in acidified (2% HNO₃ ultrapure, Merck) eluents and in mineralised soil
235 samples by ICP-AES (Spectroblue, Ametek, USA). The mineralisation of soil samples was performed
236 in DigiPREP MS system (SCP Science) at 95°C using three successive steps: 30 min with nitric acid
237 (Suprapur 65%, Merck) followed by 30 min with hydrogen peroxide (30 % AnalaR Normapur, VWR)
238 and finalised by 15 min with hydrochloric acid (37%, Fisher Scientific, Analytical grade).

239

240 PAHs and PCBs in dissolved phase were extracted by solid phase extraction (SPE) on Chromabond
241 C18 6-mL 2000-mg cartridge (Macherey-Nagel) with an AutoTrace SPE Work Station (Caliper Life
242 Sciences, USA). PAHs and PCBs in the particulate phase were extracted by Multiwave 3000
243 microwave (Anton Paar, Austria). Both types of samples were quantified using a gas chromatograph
244 (Thermo Focus GC) coupled with a mass spectrometer (Trace DSQ, Thermo Electron Corporation,
245 USA) in single ion monitoring (SIM) mode. A standard mixed containing 16 PAHs (SV Calibration
246 Mix #5/610) was supplied from Restek. An internal standard mix (PAH-Mix 31) containing 5
247 deuterated PAHs, an additional internal standard (pyrene-d10), a mixed standard containing 15 PCB
248 congeners, and 3 additional PCBs used as internal standards were purchased from LGC Promochem.
249 Analytical details for PAHs and PCBs can be found elsewhere (Bressy et al. 2011).

250

251 Enrichment factors were calculated as a ratio of trace metal mass to iron mass or as organic
252 micropollutant compound mass to organic carbon mass, compared to equivalent ratio of a reference
253 material according to Bern et al. (Bern et al. 2019).

254

255 Statistical analysis of data was conducted using the R environment (RFSC 2019) and XLSTAT
256 (Adinsoft 2018).

257

258

259

260

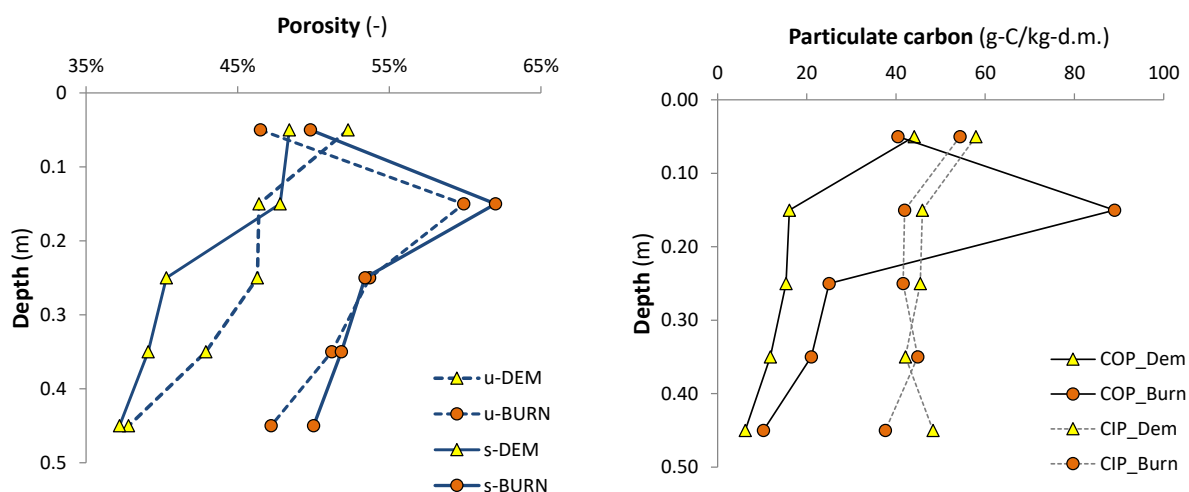
261 **Results and discussions**

262

263 **Soil contamination**

264 Based on the particle size distributions, using the diagram of Pourbey, the DEM samples can be
 265 classified, in the range of silty sand soils and the BURN samples in the silty loam soils. While the
 266 DEM soil showed increasing silt content with depth, no significant modification of vertical
 267 distribution could be observed for the BURN soil. The dry bulk density increased with depth for both
 268 types of soil, varying from 1.2 g cm^{-3} at the surface to 1.5 g cm^{-3} at 50-cm depth. Due to the presence
 269 of incompletely buried waste in the second sublayer of the BURN soil, its profile showed a peak of
 270 porosity and particulate carbon at 15-cm depth (Figure 3). The difference between the two soil types
 271 was even greater by considering the (high) proportion of coarse particles ($>2 \text{ mm}$) in the DEM soil
 272 (Table 1). The loam and silt-loam classes (Clapp and Hornberger 1978) have typically a permeability
 273 of 10^{-6} m s^{-1} , ranging between 10^{-7} m s^{-1} for pure silt to 10^{-5} m s^{-1} for sandy loam (Dunne and
 274 Leopold 1978; Dingman 2015). Due to the brick fraction and stone content in the DEM soil as
 275 observed in situ, the conductivity measured by the Guelph permeameter in the field was around $5 \cdot 10^{-5}$
 276 m s^{-1} , i.e. higher than the superior limit of 10^{-5} m s^{-1} for sandy loams. The average values of general
 277 parameters for both types of soils are given in Table 1.

278



279

280 **Fig. 3** Reconstituted porosity and particulate carbon profile in the experimental columns

281

Table. 1 Soil characteristics (n=10)

	Field			Column						
	d < 2 mm (%)	2 < d < 10 mm (%)	d > 10 mm (%)	Humidity (%)	Permeability (m s ⁻¹)	Porosity (%)	dry density (g cm ⁻³)	VS (%)	POC (%)	PIC (%)
DEM	55.0	24.4	20.6	13.8	5.10 ⁻⁵	43.8	2.46	5.1	1.9	4.8
<i>std</i>	5.0	7.0	6.8	2.0		5.1	0.18	2.0	1.0	1.0
BURN	88.6	7.6	3.8	20.6	n.d.	52.6	2.80	8.6	3.7	4.4
<i>std</i>	4.0	3.0	3.0	4.0		5.0	0.24	3.0	3.0	1.0

VS volatile solids, POC particulate organic carbon, PIC particulate inorganic carbon, *std* standard deviation

283

284

285

286

287

288

289

290

291

292

293

294

295

296

297

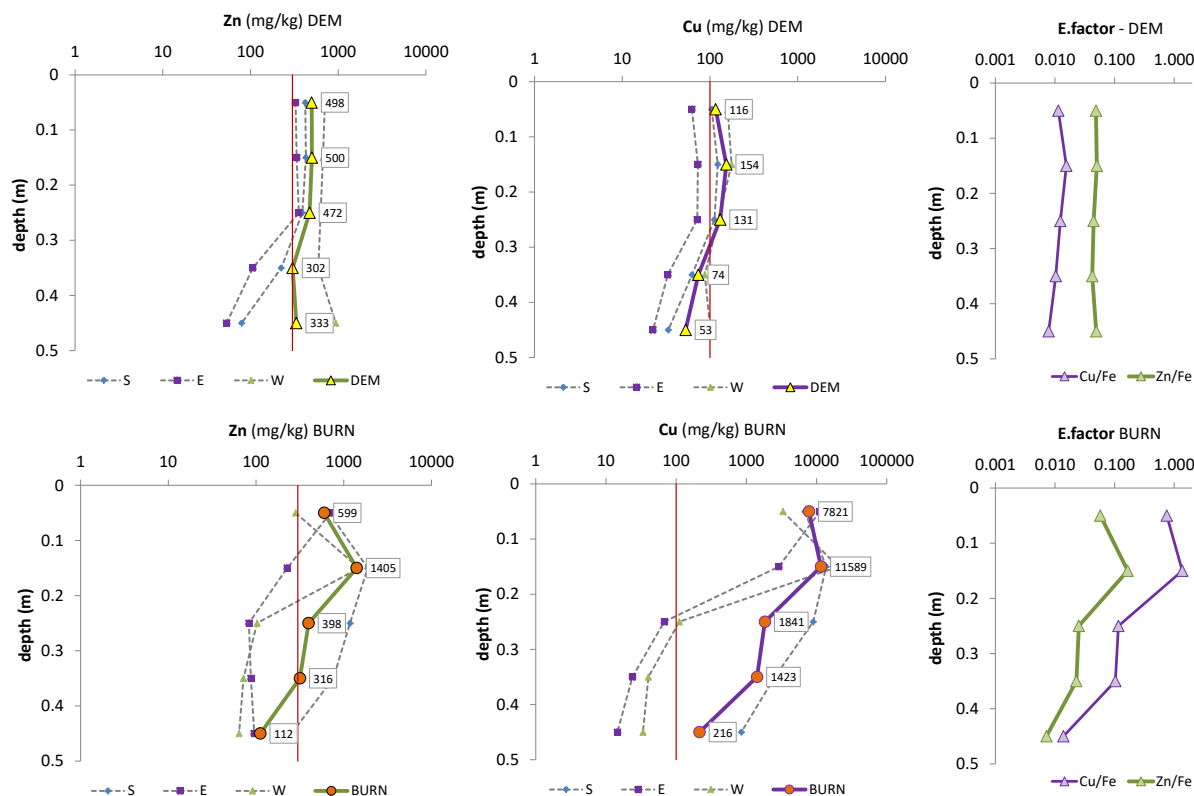
298

299

300

301

The results of X-ray fluorescence analysis (Figure 4) and organic contaminants analysis (Figure 5) confirmed that both zone are highly contaminated and exceeding the French environmental standards (Legifrance 1998; MEDDM et al. 2009). The values found are in the range of that found during the environmental screening in 2013 (Figure 1) (Guittard and et al. 2013). As expected, the BURN zone exhibited high levels of PAH (up to 39.9 mg kg⁻¹) and copper (53 to 154 mg kg⁻¹). Surprisingly also, high levels of lead and zinc (1623 and 316 g kg⁻¹ in average, respectively) were found in this zone, even higher than in the demolition zone (DEM) (Table 2). The high lead concentrations accompanied by antimony indicate a possible activity of retreatment of lead–acid batteries (Jin et al. 2015). Because of waste burning, the BURN zone was principally polluted in the upper 30 cm, and deeper layers contained natural sediments (silt) without any trace of physical anthropogenic perturbation. The DEM zone showed traces of anthropogenic pollution over the whole depth in the form of bricks, plastic and iron parts and presented therefore a minor vertical gradient as compared to the BURN zone. Iron and manganese concentrations did not show any vertical variation (data not shown). Iron concentration was higher in the BURN zone soil than in the DEM zone soil (7.2 and 4.4 g kg⁻¹, respectively) DEM and manganese concentrations were similar in both soils (about 0.1 g kg⁻¹). Compared to natural values of enrichment of 0.025 for Zn/Fe and 0.004 for Cu/Fe (Baize 2000) the DEM factor is a double, and that of copper in BURN soil is a hundred fold.

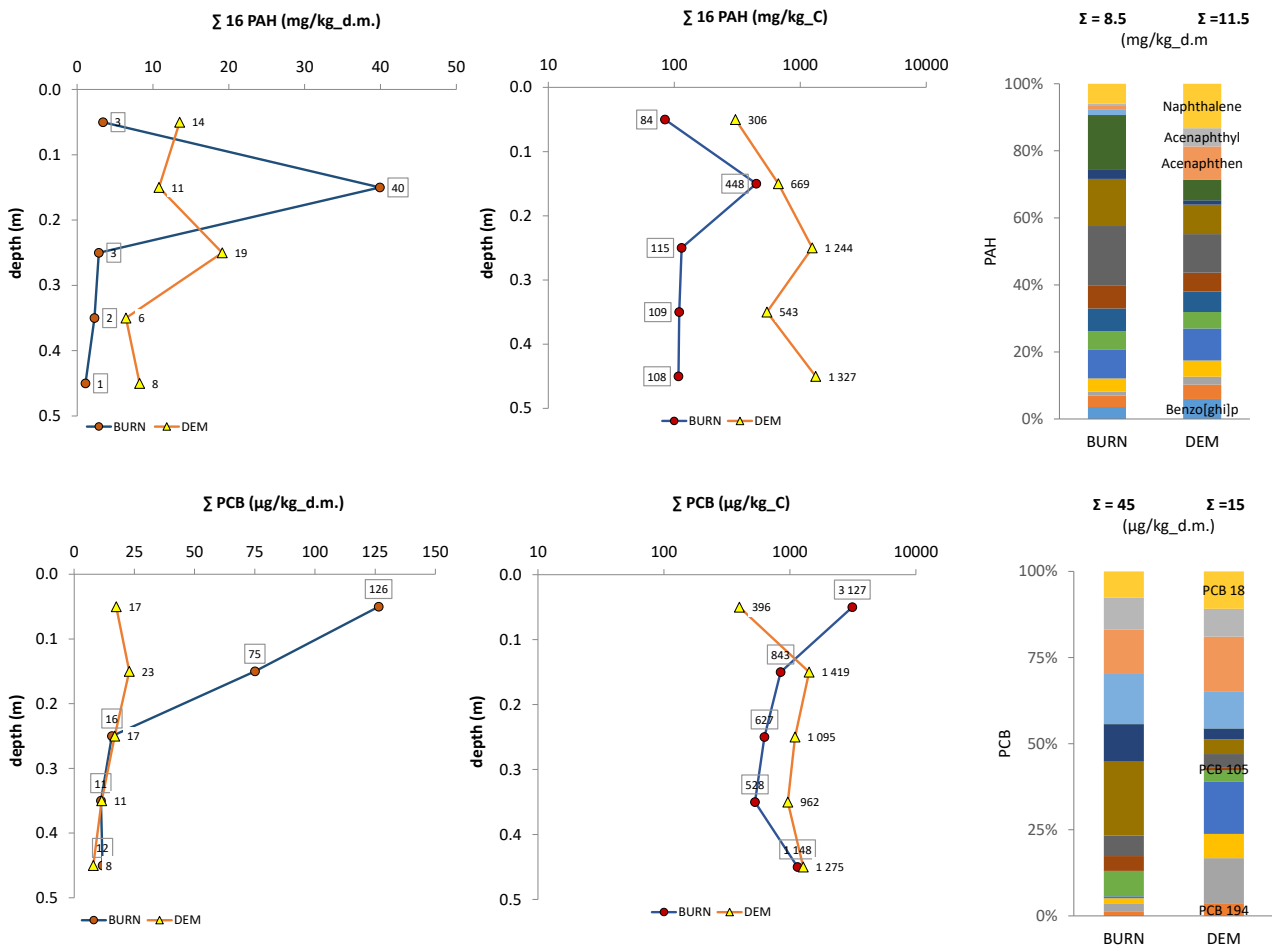


302

303 **Fig. 4** DEM zone on the top and BURN below. Zinc and Copper profiles of the fraction < 2 mm as
 304 found in the brownfield, showing the spatial heterogeneity of the pollution: south (S), east (E) and
 305 west (W) of the pollution spot centre. Solid line represents the column composite used for the column
 306 experiments. The vertical red line indicates the French limits for wastewater sludge amendments of
 307 agricultural land. For both, trace metal enrichment factors are shown.

309 As expected, beside trace metals, the brownfield was also contaminated by organic pollutants like
 310 PAH and PCB (Figure 5). The burning zone (BURN) was more contaminated especially in the top
 311 layers than the zone containing demolition material (DEM). The average contamination observed of
 312 around tenth of mg kg^{-1} of total PAH is below the range of industrial contamination of 100 to 1000
 313 mg kg^{-1} often mentioned in the literature (Crone 2001; Wang et al. 2010). However taking median
 314 values for arable land of $0.7 \text{ mg kg}_{\text{DW}}^{-1}$ (Motelay-Massei et al. 2004; Holoubek et al. 2009) as
 315 background value, even the underground of BURN zone should be considered as contaminated,
 316 classifying the whole soil profile as urban or as industrial. Normalisation with carbon showed that
 317 DEM soil was 10 times more polluted than the BURN soil.

318
 319



320
 321

322 **Fig. 5** Vertical profile of 16 PAH and their composition (above) and the equivalent of 18 PCB (below)
 323 for the two types of soil as used in the test columns. The bar charts have the components classified
 324 from the lowest molecular weight on the top (e.g. naphthalene and PCB 18) to the highest on the
 325 (e.g. benzo[ghi]perylene and PCB 209).

326

327 Like PAH, the PCBs were mainly present in the BURN soil, though more at the surface. Compared
 328 to levels of 10-20 mg kg⁻¹ found in rural areas in the Seine river basin (Motelay-Massei et al. 2004)
 329 the PCB levels of the upper soil of the BURN zone (up to 126 mg kg⁻¹) can be characterised as
 330 industrial pollution. The PCB distribution indicates a possible contamination with Aroclors as could
 331 be present in electric and electronic equipment (ATSDR and USDHHS 2000).

332
 333 The different PCB and PAH distributions between the two zones, especially if normalised by organic
 334 soil carbon concentrations, demonstrate that the type of contamination is different from one zone to
 335 another and is characteristic of the activity in each zone.

336
 337 **Table. 2** The micropollutant concentrations of soils used in the column experiments
 338

Zone		DEM	BURN
Species	Unit	Average	Average
Al	mg kg ⁻¹	2389	8734
Cd	mg kg ⁻¹	1.512	1.630
Co	mg kg ⁻¹	0.898	1.377
Cr	mg kg ⁻¹	9.760	17.77
Cu	mg kg ⁻¹	31.88	1798
Fe	mg kg ⁻¹	4420	7181
Mn	mg kg ⁻¹	103	159
Mo	mg kg ⁻¹	1.012	0.792
Ni	mg kg ⁻¹	3.490	5.716
Pb	mg kg ⁻¹	199	1623
Sb	mg kg ⁻¹	<1	19.94
Zn	mg kg ⁻¹	167	316
Benzo(a)pyrène	mg kg ⁻¹	0.57	0.47
Dibenzo(ah)anthracène	mg kg ⁻¹	0.27	0.10
Total ∑16 PAH	mg kg ⁻¹	11.5	8.52
Total ∑16 PAH /C	mg kg-C ⁻¹	735	145
PCB52	µg kg ⁻¹	0.60	10.32
PCB180	µg kg ⁻¹	1.92	1.22
Total ∑18 PCB	µg kg ⁻¹	15.30	48.02

Bulk density weighted averages ($n=5$). Arsenic and Mercury < 1 mg kg⁻¹

339 Leaching experiments

340

341 Concentrations

342 Concentrations of global parameters (pH, conductivity, turbidity, DOC, UV absorbance and
 343 fluorescence indexes), trace metals and organic pollutants were measured in the dissolved phase of
 344 the column effluents collected under each hydraulic regime (i.e. unsaturated percolation to simulate
 345 rainfall and saturated elution to simulate river flooding) (table 3). Artificial rain and river water
 346 contained appreciable amounts of total PAH (209 and 895 ng L⁻¹, respectively) and PCB (7.2 and 2.6
 347 ng L⁻¹, respectively) but limited concentrations of trace metals. High concentrations of Ca and Mg
 348 were present in all effluent samples (>100 mg L⁻¹). Several metals like Cr, Ni, Pb and Fe were not
 349 detected in the dissolved fraction of leachates, though all of them were present in the soil matrix (table
 350 2). Neither As nor Hg was detected in soils and leachates. The Zn levels were the highest in the DEM
 351 column percolated with artificial rain (356.9 µg L⁻¹) and were in the range of Zn roof runoff (Gromaire-

352 Mertz et al. 1999). Similar levels of Zn in soil leachates were found by Rennert et al. (2010) in
353 comparable experimental set-up. Significantly higher concentrations of Co, Cu and Mo were observed
354 under saturated conditions (s-DEM and s-BURN columns) compared to unsaturated percolation
355 (u-DEM and u-BURN columns). In the saturated conditions, these levels were also accompanied by
356 higher concentration of Mn, which may be due to the activity of manganese-reductive bacteria
357 reducing manganese oxides and releasing associated trace metals. Such process has already been
358 observed in soils and anaerobic sediments and was attributed to the iron- and manganese-reductive
359 bacteria. Cu and Zn showed a low solubilisation because they were probably not associated with
360 oxides. Indeed, several authors (Bousserrhine et al. 1999; Gounou et al. 2010; Harris-Hellal et al.
361 2011) have shown that in temperate soils, the organic matter constitutes the more important carrier
362 phase for Zn and Cu than iron- and manganese oxides.

363
364 The absence of ferrous iron in collected solution can be explained by the set-up, whereby effluent
365 exposed to ambient air was collected once a day and by the precipitation of solubilised iron given the
366 high pH of the solution (Bousserrhine et al. 1999). This process was confirmed by turbidity increase
367 and total iron concentration. The low solubilisation of manganese and associated metals in unsaturated
368 columns can be explained by the absence of anaerobic conditions necessary for the functioning of
369 reducing bacteria or the low activity of these bacteria.

370
371 As described by Lovley and Phillips (1986); Bousserrhine et al. (1999); and Gounou et al. (2010), the
372 reductive bacterial activity of iron and manganese is often associated with fermentation metabolism
373 producing organic acids. This metabolism probably explains the increase of DOC in the saturated
374 column where a solubilisation of trace metals was observed. None of the trace metals detected in the
375 leachate infringes the French environmental limits, nor for wastewater discharge nor for raw water for
376 drinking water supply (Legifrance 2007, 2012).

377
378 The concentrations of organic micropollutants (PAHs and PCBs) in the eluents were situated between
379 roof (Gromaire et al. 2014) and road runoff in the Paris metropole (Gasperi et al. 2010, 2012). Despite
380 the high levels in the soil, the total PAH and PCB concentrations in column effluents were even lower
381 than in the waters supplied, which indicates that these compounds were not released, but partially
382 adsorbed onto soils during percolation.

383
384 This can be explained by their relatively low solubility, which decreases with increasing molecular
385 weight. PAHs are likely bound to organic matter such as humic acid, and the binding capacity of
386 humic acid is highly dictated by protonation/deprotonation. The structure of humic acid is relatively
387 labile and the number of binding sites will depend on the pH of the solution. Schlautman and Morgan
388 (1993) showed that the binding capacity of humic acid for PAHs would increase as the pH decreases.
389 Thus, considering the relatively high pH of the solution ($\text{pH} \cong 8$), the PAHs will remain rather bound
390 to the solids than pass to the pore water solution by binding to dissolved organic matter. Another
391 important inorganic parameter that affects PAH solubility may be the 'salting-out' effect whereby the
392 PAH solubility decreases as the salt concentrations increase (Oh et al. 2013). The high conductivity
393 of the leachate, especially in unsaturated conditions, supports this hypothesis. Both effects contribute
394 not only to the retention of PAHs in the soil but also to the adsorption of PAHs present in the eluent
395 (Walsh et al. 2005).

396
397

398
399

Table. 3 Average concentrations of global parameters, trace metals and organic micropollutants in artificial rain, river water and the column effluents in dissolved fraction

		<i>LOD</i> (*)	Art. Rain	River water	u-DEM	s-DEM	u-BURN	s-BURN
Hydraulic cond.	M s ⁻¹		-	-	7.5E-06	8.3E-06	1.7E-06	2.0E-06
pH	-	0.05	6.96	8.03	7.65	7.74	7.78	7.88
Conductivity	mS cm ⁻¹	0.01	0.04	0.519	2.55	2.57	0.98	0.94
Turbidity	NTU	0.1	0.49	0.97	1.52	75.12	1.23	1.40
COD <i>t=t</i>	mgO ₂ L ⁻¹	2	<LOD	3.3	6.94	14.54	3.43	4.24
DBO ₅ <i>t=t</i>	mgO ₂ L ⁻¹	0.5	<LOD	3.5	1.8	6.0	0.7	1.6
DOC	mgC L ⁻¹	0.1	0.10	2.0	9.10	17.31	5.02	4.72
SUVA	L mgC ⁻¹	0.1	1.00	2.65	4.00	2.70	2.14	2.06
HIX	-	-	0.22	3.49	15.28	7.52	6.99	9.28
BIX	-	-	0.87	0.77	0.59	0.60	0.88	0.87
Al	µg L ⁻¹	8.0	17.10	9.77	18.3	19.0	21.9	21.7
Co	µg L ⁻¹	0.42	<LOD	<LOD	<LOD	5.19	<LOD	<LOD
Cu	µg L ⁻¹	1.2	<LOD	<LOD	7.12	16.4	<LOD	<LOD
Mg	µg L ⁻¹	5.5	396	3875	7296	7789	5069	5749
Mn	µg L ⁻¹	11	12.35	11.15	1114.0	6826.9	183.7	490.4
Mo	µg L ⁻¹	4.5	11.20	8.23	11.5	25.2	5.53	8.16
Sb	µg L ⁻¹	7.5	<LOD	<LOD	<LOD	<LOD	<LOD	52.8
Si	µg L ⁻¹	2.7	1586	1944	13683	12195	5634	5099
Zn	µg L ⁻¹	2.6	31.01	37.59	356.9	108.6	26.8	33.7
DBahA(**)	µg L ⁻¹	0.1	0.125	0.115	0.106	0.087	0.182	0.211
Σ16 PAH	µg L ⁻¹	2	209	895	118	199	185	172
PCB52	µg L ⁻¹	0.1	1.084	0.188	0.279	0.173	0.256	0.178
Σ18 PCB	µg L ⁻¹	0.1	7.239	2.581	4.028	3.033	2.772	2.324

u-DEM, demolition waste percolated by artificial rain; s-DEM, demolition waste, saturated and eluted with river water; u-BURN, river bed contaminated by electronic equipment burning, percolated by artificial rain; s-BURN, contaminated river bed, saturated and eluted with river water. The river contained 34 mgSO₄ L⁻¹ and 18 mgNO₃ L⁻¹, while the rain contained 1.32 and 1.22 mg L⁻¹, respectively. **dibenzo(ah)anthracene

**LOD* limit of detection; Cr: 1.1 µg L⁻¹; Fe: 1.3 µg L⁻¹ and Pb: 4.8 µg L⁻¹ are not shown as all values were below *LOD*

400

401 The usual evolution for long-term columns experiments under aerobic condition is a decay of the
 402 component concentration in the leachate (Cappuyns and Swennen 2008; Naka et al. 2016). This can
 403 be globally seen with conductivity and DOC in Figure 6. However, the intermittence of hydraulic
 404 regimes applied (percolation followed by a longer rest period) combines the physico-chemical
 405 processes like desorption and dissolution with microbiological transformation. For example, under
 406 flooding conditions, the dissolution processes, illustrated by turbidity and conductivity, are
 407 superposed in the beginning by bacterial reduction processes resulting in a stronger metal release.
 408 Figure 6 illustrates the influence of hydraulic conditions on the organic matter release especially for
 409 the DEM soil, where an initial fast DOC increase can be observed under saturated conditions and the
 410 saturated release of 17.3 mgC m⁻² mm⁻¹ was thereby 47% higher than the unsaturated one. For the
 411 BURN soil, there was no difference. This difference might be due to higher mineralisation rate in the
 412 anoxic conditions as was observed by other authors (Bastviken et al. 2004). This process was
 413 accompanied by aromaticity (HIX) increase. In BURN soil, it was faster than in DEM soil probably
 414 due to leaching of burned material in the first and humic substances in the latter (Huguet et al. 2009,
 415 2010).

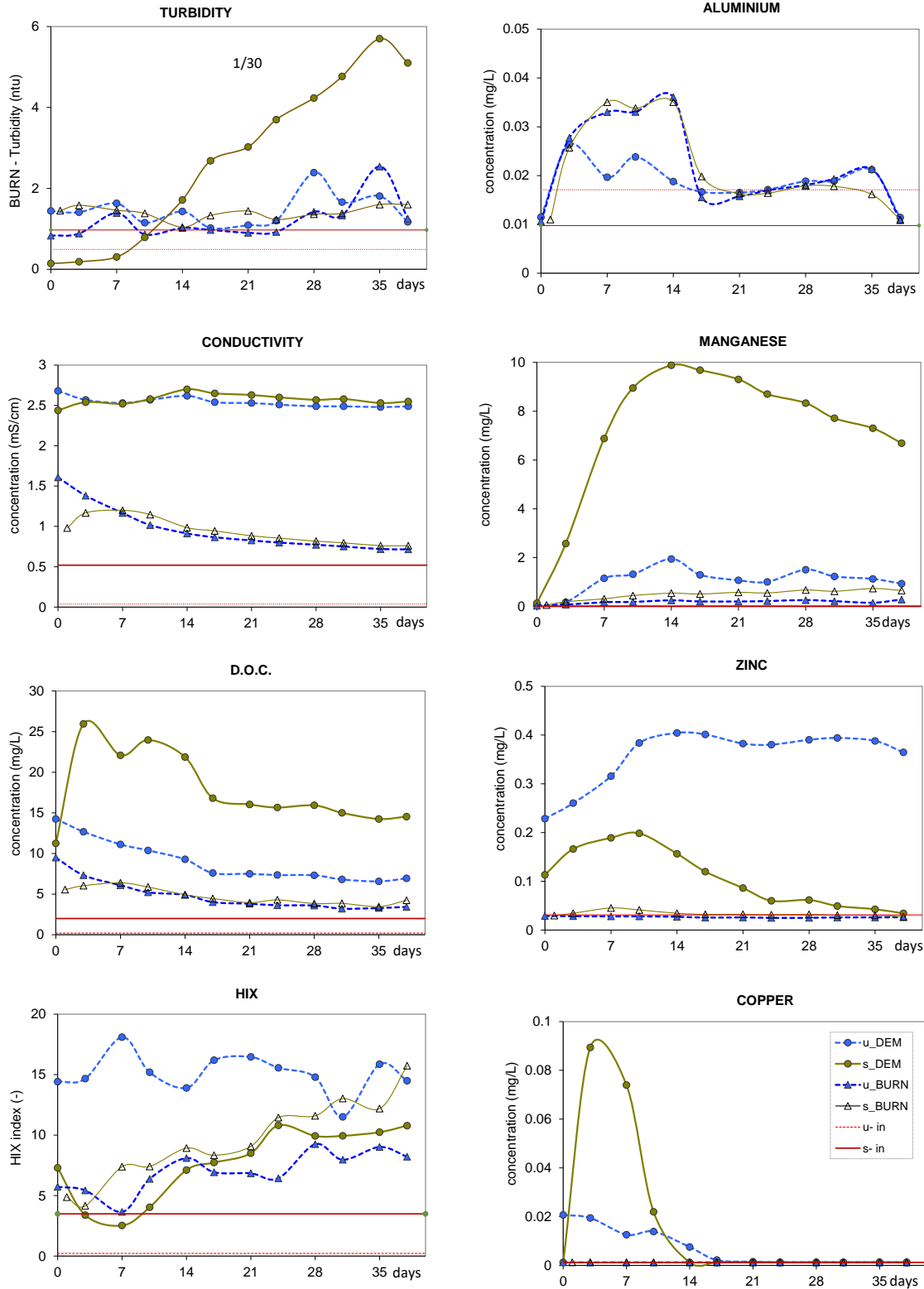
416

417 Though the heavy metal content was much higher in the BURN soil than in the DEM soil, the levels

418 of Cu and Zn were lower in the BURN zone effluents than in the DEM effluents. This could be
419 explained by the difference in soil composition, trace metal association to soil components and
420 bacterial activity. Cu and Zn were probably more associated to iron and manganese oxides in DEM
421 samples than in BURN ones. The polluted upper silt soil released only slowly the heavy metals due
422 to presence of carbonates (higher pH), better retaining the pollution before passing to lower levels.
423 An initial increase of Cu was observed due to liberation of easily bound metals linked to organic
424 matter, alumino-silicates and or Fe/Mn hydroxides, followed by decay (Figure 6). Similar results were
425 reported by Gounou et al. (2010) showing that in anaerobic sediment, the bacterial reduction of iron
426 oxides was concomitant with trace metal solubilisation. The flux of zinc and copper in the recomposed
427 DEM soil seemed therefore to be related to organic matter release ($r^2=0.88$, respectively, $r^2=0.98$,
428 $p>0.05$). The gradual transformation of organic matter can be seen from the increase of the HIX
429 fluorescence index. Under saturated conditions, zinc and copper were thereby more linked to the
430 aromatic components HIX ($r^2=0.95$, respectively, $r^2=0.82$, $p>0.05$) than BIX. No correlation was
431 observed with HIX under unsaturated conditions. This behaviour was not observed for the BURN soil.
432 Both metals showed correlation with manganese under aerobic conditions ($r^2>0.6$, $p>0.05$) for DEM
433 and BURN soil but not under the anoxic conditions.

434
435 The hydraulic conditions influenced the redox conditions and therefore the metal release. The major
436 indicator of redox conditions is iron, not soluble under oxic conditions (unsaturated percolation), but
437 soluble under anoxic conditions (saturated flow). No dissolved iron was directly detected in the
438 leachates (Table 3); however, iron was detected in colloidal form in the s-DEM effluents after 2 days
439 of experiment and stabilised after 10 days at a level of 9.7 mg L^{-1} . Dissolved iron leached from the
440 saturated column under anoxic conditions and precipitated afterwards as colloids in the sampling
441 bottle, where it was exposed to aerobic conditions. This precipitation of iron in amorphous form has
442 been widely described for anaerobic environments with high pH and identified as the reason for trace
443 metal precipitation (Bousserrhine et al. 1999; Gounou et al. 2010; Harris-Hellal et al. 2011). The
444 initial iron solubilisation was also accompanied by Cu and Zn release. 90% of copper and 20% of zinc
445 were hereby present in particulate form, trapped in the colloids. The decrease of Al, Cu and Zn
446 concentrations at the end of the experiment under saturated conditions can be explained by the
447 formation of metallic sulphides following bacterial sulphate-reductive activity as has been reported
448 by Bousserrhine and Gounou (Bousserrhine et al. 1999; Gounou et al. 2010).

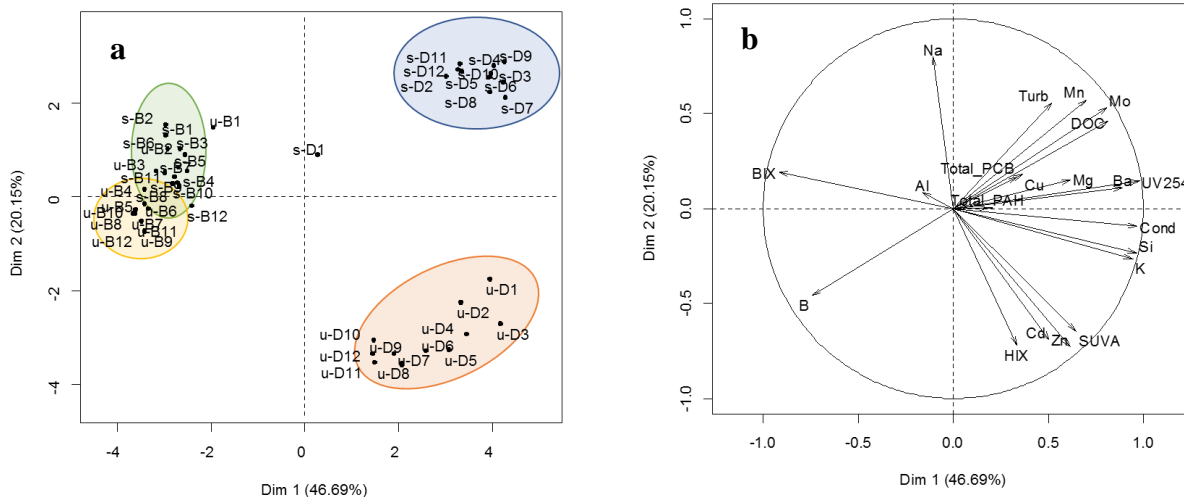
449
450 Regarding PAHs and PCBs, there was no significant trend in the leachate concentrations of the four
451 columns. Comparable levels of PAHs were found by Azah et al. (2017) in batch extraction of storm
452 water sediments with artificial rain. Nevertheless, the dust used had a PAH content ten times lower
453 than the soils HC and MX. The difference is probably due to the hydraulic conditions of batch
454 experiments, high specific surface of dust particles and the acidity of rain, used by Azah (2017).



455
 456 **Fig. 6** Evolution of leachate concentrations ($< 0.45 \mu\text{m}$). Straight red lines represent the initial eluent
 457 concentration (rain and river water). The dashed lines correspond to experiments with artificial
 458 rainwater, and the solid lines corresponds to experiments with river water, whereby the dots represent
 459 the soil recomposed from contaminated demolition waste (DEM) and triangles represent burning zone
 460 soil (BURN). The iron, not shown, was only detected in the saturated DEM soil, at same level as
 461 manganese but in the form of colloids
 462

463 **Effect of hydraulic conditions on pollutant release**

464 **PCA** A principal component analysis (PCA) was performed to better understand the relationships
 465 between all measured parameters. The PCA results show that the four types of columns can be clearly
 466 differentiated according to the soil types and hydraulic conditions, based on the whole set of analytical
 467 results (Figure 7).
 468



469 **Fig. 7** PCA for the overall set of concentration data. D, DEM; B, BURN. **a** scores plot; **b** loadings
 470 plot
 471

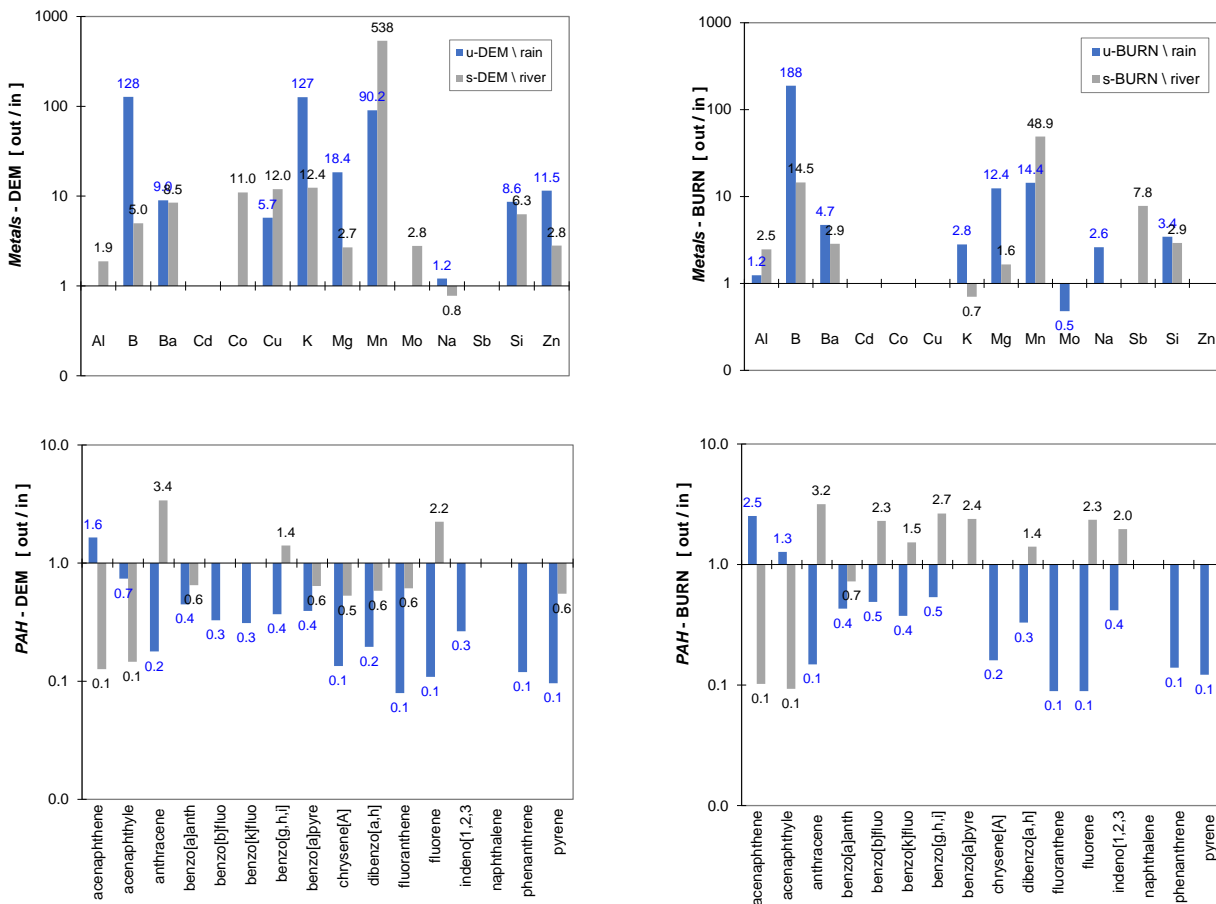
472
 473 PCA analysis differentiated clearly by the first dimension, BURN soil on the left (negative portion of
 474 the X axis) and the DEM soil on the right side (positive portion of the X axis). The first dimension
 475 was mainly driven by the conductivity (capacity of dissolution), organic matter (DOC) and its
 476 aromaticity type (UV254, BIX) as well as the metal content. The samples from the BURN zone were
 477 characterised by higher values of BIX fluorescence index and boron and sodium concentrations, while
 478 the samples from the DEM zone were characterised by higher conductivity, DOC, copper, manganese
 479 and zinc, as well as the dibenzo(a)anthracene and benzo(a)anthracene inter alia.

480
 481 The second PCA dimension was mainly driven by sodium concentration followed by HIX index and
 482 trace metals Zn and Cd, thus indicating that the flooding condition favoured the release of sodium in
 483 leachates. The differentiation between the two hydraulic conditions was more pronounced for the
 484 DEM samples. From these samples, Mn and Mo were mainly released under flooding conditions,
 485 while Cd and Zn releases were favoured by the rainfall hydraulic regime.

486
 487 **Fluxes** To evaluate the overall contribution of hydraulic conditions and types of soil to the pollutant
 488 release, total fluxes were calculated from concentrations and flows. The incoming fluxes entering the
 489 columns were compared to the outgoing fluxes (Figure 8). Three types of behaviour could be
 490 observed: (i) no leaching whereby the outgoing flux was globally equal to the applied flux (Co, Cd,
 491 Al, Na); (ii) a medium leaching, whereby outgoing flux was globally ten times the incoming flux
 492 (Cu, Si, Zn); and (iii) a pronounced leaching of metals above quotient of 100 (Mn, K, B).

493
 494 The rainfall unsaturated condition had a stronger leaching effect than the saturated condition regarding
 495 Zn, Mg, K, and B. This behaviour was even more pronounced for the DEM soil than for the BURN
 496 soil. The rain condition maintains an open soil structure with presence of oxygen and that river
 497 flooding condition tends to modify the soil structure lowering the permeability and creating anoxic

498 conditions. The anoxic conditions may diminish the solubility of metals by forming sulphides, which
 499 could explain the higher release of several metals (Zn, Mg, K, B) under unsaturated conditions. On
 500 the contrary, under reducing conditions, high-valent iron and manganese present in soils are
 501 reductively dissolved via a number of alternative abiotic and microbial pathways (Roden and Wetzel
 502 2002). Fe(III) can act as a terminal electron acceptor during microbially mediated decomposition of
 503 organic matter, forming soluble ferrous ion (Fe^{2+}) (Lovley and Phillips 1986; Bousserhine et al.
 504 1999). This picture becomes more complex, if we take into account the presence of nitrate and sulphate
 505 in the river water and Fe^{2+} and Mn^{2+} as potential electron donors making their oxidation possible,
 506 through nitrate reduction (Pyzola 2013). The higher fluxes of Fe and Mn and lower flux of Zn in the
 507 s-DEM leachate (saturated conditions), compared to the u-DEM leachate (unsaturated conditions), are
 508 in accordance with these processes.
 509



510
 511
 512 **Fig. 8** Retention and release of different micropollutants as the ratio of the outcoming to incoming
 513 flux. A value below 1 means retention and value above 1 means release. Values between 0.8 and 1.2,
 514 estimates are not significantly different from 1 and are not shown. PCBs are not shown as all species
 515 were retained in both substrates. Saturated conditions in grey, unsaturated in blue
 516

517 As described before, the BURN soil exhibited the highest contamination by metals, but its natural clay
 518 structure and high organic matter content immobilised the pollution and presented *in fine* little
 519 leaching in the different hydraulic conditions. The differences between the saturated and unsaturated
 520 flows regarding the leaching of metals were rather due to the existence of different redox conditions
 521 than to the difference in residence time (i.e. ratio of saturated pore volume and flow). Neither the
 522 higher water content of saturated columns compared to unsaturated nor the higher porosity of BURN

523 soil compared to DEM soil impacted the release of micropollutants. The low importance of flow
524 velocity was also reported by Naka (Naka et al. 2016).

525

526 Contrary to metals, the change in hydraulic conditions had a clear impact on the PAH retention. The
527 retention of all PAH was high (flux ratio always < 1 except for anthracene and fluorene) under
528 saturated conditions in both the DEM and the BURN soils (s-DEM and s-BURN in Figure 7). In
529 saturated conditions (i.e. river flood condition), PAH flux ratio was closer or higher to 1, especially
530 for the BURN soil (i.e. u-BURN). These results indicate that the rain (acidity), combined with
531 unsaturated flow, created conditions favourable for retention of PAH, while in saturated conditions,
532 PAH were more released especially in the BURN soil, most probably due to desaturation of the
533 burning layer. PCB exhibited a similar behaviour than PAH with a lower difference between the two
534 hydraulic conditions.

535

536 Pollutants fluxes can also be expressed in $\text{g m}^{-2} \text{year}^{-1}$ or $\text{kg ha}^{-2} \text{year}^{-1}$. If we focus on zinc and
537 copper, there was only a net flux from the DEM soil. Taking the average annual precipitation on the
538 region of 650 mm, dissolved zinc showed a flux of $2.1 \text{ kg ha}^{-2} \text{year}^{-1}$ for the rainfall condition
539 (u-DEM) decreasing to $0.36 \text{ kg ha}^{-2} \text{year}^{-1}$ for the river flood condition (s-DEM). Compared to the
540 annual atmospheric deposition of zinc in the Paris region of 0.45 to $1.2 \text{ kg ha}^{-2} \text{year}^{-1}$ (Azimi et al.
541 2005), these values may impact significantly the background levels for zinc. Dissolved copper
542 behaved differently with $0.038 \text{ kg ha}^{-2} \text{year}^{-1}$ for u-DEM increasing to $0.078 \text{ kg ha}^{-2} \text{year}^{-1}$ for s-DEM.
543 These fluxes were significantly higher if we take into account the flux of particulate copper
544 associated to iron, and would be close to values of the atmospheric deposition of 0.1 to 0.2
545 $\text{kg ha}^{-2} \text{year}^{-1}$ reported by Azimi (Azimi et al. 2005) and Gasperi (Gasperi et al. 2014).

546

547 **Conclusions**

548

549 The studied soils were moderately to strongly polluted, exceeding the French environmental limits
550 (MEDDM et al. 2009). The DEM soil, marked by demolition disposal over the whole depth, was
551 coarser with higher permeability. The BURN soil was finer and only impacted in the upper soil, with
552 undisturbed layers below. The DEM soil was moderately polluted with trace metals over the whole
553 depth, while the BURN soil was extremely polluted (Zn, Cu and Pb of several g kg^{-1} with pronounced
554 presence of PAH and PCB) only in the first 20 cm of the soil profile.

555

556 The results showed that the intermittence of hydrological regime increased the pollutant release
557 compared to continuous exposition, though the type and structure of soil were of greater importance
558 than the condition of saturation applied. The leachates of the DEM soil were characterised by higher
559 conductivity and DOC content, indicating dissolution and desorption as key processes in pollutant
560 release. Though the BURN soil was 10 times more contaminated with trace metals than the DEM soil,
561 only the latter released copper, zinc and cobalt in significant amounts. Iron- and manganese-reducing
562 bacteria were implicated in the solubilisation of trace metals under anaerobic conditions through the
563 production of soluble iron and manganese oxides and the release of associated metals. The
564 concentrations of pollutants in the leachates were close to those of road runoff and for zinc and copper
565 far above the European standards for receiving water bodies (CEE 2008). According to literature
566 (Seidl et al. 1998; Baun et al. 2008), their peak concentration could eventually generate an acute
567 exposition level if directly released to aquatic ecosystems.

568

569 Statistical analysis of the data showed more pronounced differences between the two soil types than
570 between the two hydrological regimes studied (i.e., rainfall and river flooding). Hydrology was still a
571 significant driver especially for the DEM soil and to a lesser extent for the BURN soil. Unsaturated
572 conditions (rainfall) favoured dissolution of silicates and zinc release, while the application of

573 saturated conditions (river flooding) created reductive environment liberating iron and manganese and
574 most probably linked copper. PAH remained adsorbed onto soil in unsaturated conditions but slightly
575 released under saturated flow in the BURN soil. The PCB did not release. No significant relationship
576 was observed between the organic micropollutants and the organic matrix indicators (HIX, BIX and
577 aromaticity), suggesting that these parameters and the humic substances present in the soil matrix
578 were not directly linked to the behaviour of these pollutants. The only correlation for these parameters
579 was found for zinc and copper in the u-DEM soil suggesting their release under anaerobic condition
580 to be also linked to humic matter transformation.

581
582 Based on the presented leaching experiments, it can be concluded that under actual field conditions,
583 the high levels of PAHs, PCBs and trace metals present upon natural silty sedimentary soils (BURN)
584 do not present an immediate risk for the surrounding aquatic ecosystem because of strong associations
585 between organic pollutants, soil particles, metals and iron or manganese oxides. During flood periods,
586 a limited release of PAHs can be expected. On the contrary, the less contaminated demolition disposal
587 (DEM) presents a moderate risk of zinc and copper mobilisation under actual hydrological conditions
588 (i.e. rain events), doubling the atmospheric wet weather deposition. Overall, a flooding condition
589 would produce a lower risk of trace metal release than rainfall but will cause a cumulative effect.

590
591 The general implication of the results obtained is that long-term risk assessment of contained soil
592 should be done with stratified media, applying hydrological conditions (saturation, periodicity,
593 duration of exposition...) as close as possible to field conditions rather than using standard batch tests
594 with fixed L/S ratio. The approach used allowed to identify biogeochemical transformations and to
595 estimate more adequately the fluxes which could be released to the environment.

596
597 The experimental set-up showed to be adequate to study different hydrological conditions of stratified
598 soil contamination and allowed to simulate in situ conditions and obtain more realistic results than
599 batch experiments or full mixed columns. However, some improvements might improve the overall
600 sensitivity of the system, such as airtight sampling bags preventing the oxidation and transformation
601 of collected samples. Moreover, parallel measurements of auxiliary parameters like in- and outcoming
602 nitrate, sulphate and BOD5 would give better information about the existing microbiological
603 processes.

604

605 **Supplementary Information**

606 The online version contains supplementary material available at [https://doi.org/10.1007/s11356-021-](https://doi.org/10.1007/s11356-021-15491-0)
607 [15491-0](https://doi.org/10.1007/s11356-021-15491-0).

608

609 **Acknowledgements**

610 The authors acknowledge the Conseil départemental Val-de-Marne for their indispensable assistance
611 during the fieldwork and Olivier Fouché for the field permeability data.

612

613 **Author contribution**

614 Conceptualization: Martin Seidl. Methodology: Remi Mazerolle, Martin Seidl and Julien Le
615 Roux. Investigation: Remi Mazerolle and Martin Seidl. Formal analysis: Martin Seidl and Julien Le
616 Roux. Writing, original draft preparation: Martin Seidl. Writing, review and editing: Martin Seidl,
617 Julien Le Roux and Nouredine Bousserhine. Funding acquisition: Martin Seidl and Nouredine
618 Bousserhine. Resources: Martin Seidl, Julien Le Roux and Nouredine Bousserhine. Supervision:
619 Martin Seidl

620

621 **Funding**

622 The authors acknowledge the Region Ile-de-France for its financial support to the REFUJ project,
623 coordinated by Mathieu Bagard, through the partnership between research institutions and the civil
624 society (PICRI).

625

626 **Data availability**

627 All major data generated during this study are included in the published article. Complementary data
628 are available from the corresponding author on request.

629

630 **Declarations**

631 **Ethics approval** Not applicable

632 **Consent to participate** Not applicable

633 **Consent for publication** All authors consent to publish

634 **Competing interests** The authors declare no competing interests

635

636 **References**

637

638 ADEME (2014) Taux d'utilisation et coûts des différentes techniques et filières de traitement des
639 sols et des eaux souterraines pollués en France - Synthèse des données 2012.
640 [http://www.ademe.fr/sites/default/files/assets/documents/84580_rapport_taux_couts_traitem](http://www.ademe.fr/sites/default/files/assets/documents/84580_rapport_taux_couts_traitements_sols_eaux.pdf)
641 [ents_sols_eaux.pdf](http://www.ademe.fr/sites/default/files/assets/documents/84580_rapport_taux_couts_traitements_sols_eaux.pdf). Accessed 17 Feb 2016

642 Adinsoft (2018) Statistical software & data analysis add-on for Excel | XLSTAT 2020. Version
643 2018.7 Build 54791URL <https://www.xlstat.com/en/>

644 AFNOR (2002) NF EN 12457-4 - Caractérisation des déchets - Lixiviation - Essai de conformité
645 pour lixiviation des déchets fragmentés et des boues - Partie 4 : essai en bâchée unique avec
646 un rapport liquide/solide de 10 l/kg et une granularité inférieure à 10 mm (sans ou avec
647 réduction de la granularité)

648 AFNOR (2005) Qualité de l'eau, 7eme édition. AFNOR

649 APHA, AWWA, WEF, et al (2012) Standard Methods for the Examination of Water and
650 Wastewater, 22 edition. American Public Health Association, American Water Works
651 Association and Water Environment Federation, Washington, DC

652 ATSDR, USDHHS (2000) Toxicological profile for polychlorinated biphenyls (PCBs). Agency for
653 Toxic Substances and Disease Registry, Atlanta, Georgia

654 Azah E, Kim H, Townsend T (2017) Assessment of direct exposure and leaching risk from PAHs in
655 roadway and stormwater system residuals. *Science of The Total Environment* 609:58–67.
656 <https://doi.org/10.1016/j.scitotenv.2017.07.136>

657 Azimi S, Rocher V, Garnaud S, et al (2005) Decrease of atmospheric deposition of heavy metals in
658 an urban area from 1994 to 2002 (Paris, France). *Chemosphere* 61:645–651.
659 <https://doi.org/10.1016/j.chemosphere.2005.03.022>

660 Baize D (2000) Teneurs totales en « métaux lourds » dans les sols français résultats généraux du
661 programme ASPITET. *Courrier de l'environnement de l'INRA* n°39, février:39–54

- 662 Bastviken D, Persson L, Odham G, Tranvik L (2004) Degradation of dissolved organic matter in
663 oxic and anoxic lake water. *Limnology and Oceanography* 49:109–116.
664 <https://doi.org/10.4319/lo.2004.49.1.0109>
- 665 Baun A, Seidl M, Scholes L, et al (2008) Chap. 20: Application of a battery of biotests for toxicity
666 characterization of stormwater. In: Thévenot DR (ed) *DayWater: Adaptive Decision Support*
667 *System for Integrated Urban Stormwater Control*. IWA Publishers, pp 207–213
- 668 Bern CR, Walton-Day K, Naftz DL (2019) Improved enrichment factor calculations through
669 principal component analysis: Examples from soils near breccia pipe uranium mines,
670 Arizona, USA. *Environmental Pollution* 248:90–100.
671 <https://doi.org/10.1016/j.envpol.2019.01.122>
- 672 Bousserhine N, Gasser UG, Jeanroy E, Berthelin J (1999) Bacterial and chemical reductive
673 dissolution of Mn-, Co-, Cr-, and Al-substituted goethites. *Geomicrobiol J* 16:245–258.
674 <https://doi.org/10.1080/014904599270622>
- 675 Bressy A, Gromaire M-C, Lorgeoux C, Chebbo G (2011) Alkylphenols in atmospheric depositions
676 and urban runoff. *Water Science and Technology* 63:671–9.
677 <https://doi.org/10.2166/wst.2011.121>
- 678 Camobreco VJ, Richards BK, Steenhuis TS, et al (1996) Movement of heavy metals through
679 undisturbed and homogenised soil columns. *Soil Science* 161:740–750
- 680 Cappuyns V, Swennen R (2008) The Use of Leaching Tests to Study the Potential Mobilization of
681 Heavy Metals from Soils and Sediments: A Comparison. *Water Air Soil Pollut* 191:95–111.
682 <https://doi.org/10.1007/s11270-007-9609-4>
- 683 CEE (2008) Directive 2008/105/CE du Parlement européen et du Conseil du 16 décembre 2008
684 établissant des normes de qualité environnementale dans le domaine de l'eau, modifiant et
685 abrogeant les directives du Conseil 82/176/CEE, 83/513/CEE, 84/156/CEE, 84/491/CEE,
686 86/280/CEE et modifiant la directive 2000/60/CE. *Journal officiel de l'Union européenne OJ*
687 L:
- 688 Clapp RB, Hornberger GM (1978) Empirical equations for some soil hydraulic properties. *Water*
689 *Resour Res* 14:601–604. <https://doi.org/10.1029/WR014i004p00601>
- 690 Crone M (2001) Diagnostic de sols pollués par des hydrocarbures aromatiques polycycliques (HAP)
691 a l'aide de la spectrophotométrie UV. Ecole Nationale Supérieure des Mines de Saint-
692 Etienne; INSA de Lyon
- 693 Cueff S, Alletto L, Bourdat-Deschamps M, et al (2020) Water and pesticide transfers in undisturbed
694 soil columns sampled from a Stagnic Luvisol and a Vermic Umbrisol both cultivated under
695 conventional and conservation agriculture. *Geoderma* 377:114590.
696 <https://doi.org/10.1016/j.geoderma.2020.114590>
- 697 Dermont G, Bergeron M, Mercier G, Richer-Lafèche M (2008) Soil washing for metal removal: A
698 review of physical/chemical technologies and field applications. *Journal of Hazardous*
699 *Materials* 152:1–31. <https://doi.org/10.1016/j.jhazmat.2007.10.043>
- 700 Dingman SL (2015) *Physical hydrology*, 3. ed. Waveland Press, Long Grove, Ill

- 701 DRIEE (2015) Plan de gestion des risques d'inondation (PGRI) du bassin Seine-Normandie 2016-
702 2021
- 703 DRIEE (2018) Inondations - DRIEE Ile-de-France. [http://www.driee.ile-de-france.developpement-
durable.gouv.fr/inondations-r183.html](http://www.driee.ile-de-france.developpement-
704 durable.gouv.fr/inondations-r183.html). Accessed 3 Nov 2018
- 705 Du Laing G, Rinklebe J, Vandecasteele B, et al (2009) Trace metal behaviour in estuarine and
706 riverine floodplain soils and sediments: A review. *Science of The Total Environment*
707 407:3972–3985. <https://doi.org/10.1016/j.scitotenv.2008.07.025>
- 708 Dunne T, Leopold LB (1978) *Water in Environmental Planning*, 1st edition. W. H. Freeman, San
709 Francisco
- 710 ENPF (2017) Espace Naturel de la Pierre-Fitte. <https://fr-fr.facebook.com/EspaceNaturelPierreFitte/>.
711 Accessed 29 Aug 2017
- 712 Fang W, Wei Y, Liu J, et al (2016) Effects of aerobic and anaerobic biological processes on leaching
713 of heavy metals from soil amended with sewage sludge compost. *Waste Management*
714 58:324–334. <https://doi.org/10.1016/j.wasman.2016.07.036>
- 715 Gasperi J, Gromaire MC, Kafi M, et al (2010) Contributions of wastewater, runoff and sewer
716 deposit erosion to wet weather pollutant loads in combined sewer systems. *Water Research*
717 44:5875–5886. <https://doi.org/10.1016/j.watres.2010.07.008>
- 718 Gasperi J, Sebastian C, Ruban V, et al (2014) Micropollutants in urban stormwater: occurrence,
719 concentrations, and atmospheric contributions for a wide range of contaminants in three
720 French catchments. *Environmental Science and Pollution Research* 21:5267–5281.
721 <https://doi.org/10.1007/s11356-013-2396-0>
- 722 Gasperi J, Zgheib S, Cladière M, et al (2012) Priority pollutants in urban stormwater: Part 2 – Case
723 of combined sewers. *Water Research* 46:6693–6703.
724 <https://doi.org/10.1016/j.watres.2011.09.041>
- 725 Gonzalez M, Mitton FM, Miglioranza KSB, Peña A (2019) Role of a non-ionic surfactant and
726 carboxylic acids on the leaching of aged DDT residues in undisturbed soil columns. *J Soils
727 Sediments* 19:1745–1755. <https://doi.org/10.1007/s11368-018-2172-3>
- 728 Gounou C, Bousserrhine N, Varrault G, Mouchel J-M (2010) Influence of the Iron-Reducing
729 Bacteria on the Release of Heavy Metals in Anaerobic River Sediment. *Water Air Soil Pollut*
730 212:123–139. <https://doi.org/10.1007/s11270-010-0327-y>
- 731 Gromaire M-C, Lamprea-Bretauudeau K, Seidl M, Mirande-Bret C (2014) Organic micropollutants in
732 roof runoff – a study of the emission / retention potential of green roofs. In: ICUD 2014, 13th
733 International Conference on Urban Drainage, Sarawak, Malaysia, 7-12 September 2014
- 734 Gromaire-Mertz MC, Garnaud S, Gonzalez A, Chebbo G (1999) Characterisation of urban runoff
735 pollution in Paris. *Water Science and Technology* 39:1–8. [https://doi.org/10.1016/S0273-
1223\(99\)00002-5](https://doi.org/10.1016/S0273-
736 1223(99)00002-5)
- 737 Guittard A, et al. (2013) Evaluation quantitative des risques sanitaires (EQRS) Prestation codifiée
738 A320 selon NF X31-620

- 739 Harris-Hellal J, Grimaldi M, Garnier-Zarli E, Bousserhine N (2011) Mercury mobilisation by
740 chemical and microbial iron oxide reduction in soils of French Guyana. *Biogeochemistry*
741 103:223–234. <https://doi.org/10.1007/s10533-010-9457-y>
- 742 Holoubek I, Dušek L, Sáňka M, et al (2009) Soil burdens of persistent organic pollutants – Their
743 levels, fate and risk. Part I. Variation of concentration ranges according to different soil uses
744 and locations. *Environmental Pollution* 157:3207–3217.
745 <https://doi.org/10.1016/j.envpol.2009.05.031>
- 746 Huguet A, Vacher L, Relexans S, et al (2009) Properties of fluorescent dissolved organic matter in
747 the Gironde Estuary. *Organic Geochemistry* 40:706–719.
748 <https://doi.org/10.1016/j.orggeochem.2009.03.002>
- 749 Huguet A, Vacher L, Saubusse S, et al (2010) New insights into the size distribution of fluorescent
750 dissolved organic matter in estuarine waters. *Organic Geochemistry* 41:595–610.
751 <https://doi.org/10.1016/j.orggeochem.2010.02.006>
- 752 ISO (2019) ISO 21268-3 Soil quality — Leaching procedures for subsequent chemical and
753 ecotoxicological testing of soil and soil-like materials — Part 3: Up-flow percolation test
- 754 Jin Z, Zhang Z, Zhang H, et al (2015) Assessment of lead bioaccessibility in soils around lead
755 battery plants in East China. *Chemosphere* 119:1247–1254.
756 <https://doi.org/10.1016/j.chemosphere.2014.09.100>
- 757 Kafi M, Gasperi J, Moilleron R, et al (2008) Spatial variability of the characteristics of combined
758 wet weather pollutant loads in Paris. *Water Research* 42:539–549.
759 <https://doi.org/10.1016/j.watres.2007.08.008>
- 760 Legifrance (1998) Arrêté du 8 janvier 1998 fixant les prescriptions techniques applicables aux
761 épandages de boues sur les sols agricoles pris en application du décret no 97-1133 du 8
762 décembre 1997 relatif à l'épandage des boues issues du traitement des eaux usées. JORF
763 n°26 du 31 janvier 1998 page 1563
- 764 Legifrance (2007) Arrêté du 11 janvier 2007 relatif aux limites et références de qualité des eaux
765 brutes et des eaux destinées à la consommation humaine mentionnées aux articles R. 1321-2,
766 R. 1321-3, R. 1321-7 et R. 1321-38 du code de la santé publique. JORF JORF n° 31 du
767 06/02/2007 texte numéro 17
- 768 Legifrance (2012) Arrêté du 26 mars 2012 relatif aux prescriptions générales applicables aux
769 installations classées relevant du régime de l'enregistrement au titre de la rubrique n° 2710-2
770 (installations de collecte de déchets non dangereux apportés par leur producteur initial) de la
771 nomenclature des installations classées pour la protection de l'environnement - Article 35 |
772 Legifrance. JORF
- 773 Li J, Jia C, Lu Y, et al (2015) Multivariate analysis of heavy metal leaching from urban soils
774 following simulated acid rain. *Microchemical Journal* 122:89–95.
775 <https://doi.org/10.1016/j.microc.2015.04.015>
- 776 Lovley DR, Phillips EJP (1986) Organic Matter Mineralization with Reduction of Ferric Iron in
777 Anaerobic Sediments. *Appl Environ Microbiol* 51:683–689

- 778 MEDDM, DGALN, DEB (2009) Recueil de textes sur l'assainissement : Textes techniques relatifs à
779 l'épandage des boues d'épuration résultant du traitement des eaux usées domestiques.
780 Ministère de l'écologie, de l'énergie, du développement durable et de la mer (MEDDM),
781 Direction générale de l'aménagement, du logement et de la nature (DGALN) Direction de
782 l'eau et de la biodiversité (DEB) Bureau de la lutte contre les pollutions domestiques et
783 industrielles
- 784 Motelay-Massei A, Ollivon D, Garban B, et al (2004) Distribution and spatial trends of PAHs and
785 PCBs in soils in the Seine River basin, France. *Chemosphere* 55:555–565.
786 <https://doi.org/10.1016/j.chemosphere.2003.11.054>
- 787 Naka A, Yasutaka T, Sakanakura H, et al (2016) Column percolation test for contaminated soils:
788 Key factors for standardization. *Journal of Hazardous Materials* 320:326–340.
789 <https://doi.org/10.1016/j.jhazmat.2016.08.046>
- 790 Nasri B, Fouché O, Ramier D (2015) Monitoring infiltration under a real on-site treatment system of
791 domestic wastewater and evaluation of soil transfer function (Paris Basin, France).
792 *Environmental Earth Sciences* 73:7435–7444. <https://doi.org/10.1007/s12665-014-3917-y>
- 793 Oh S, Wang Q, Shin WS, Song D-I (2013) Effect of salting out on the desorption-resistance of
794 polycyclic aromatic hydrocarbons (PAHs) in coastal sediment. *Chemical Engineering*
795 *Journal* 225:84–92. <https://doi.org/10.1016/j.cej.2013.03.069>
- 796 Pot V, Benoit P, Menn ML, et al (2011) Metribuzin transport in undisturbed soil cores under
797 controlled water potential conditions: experiments and modelling to evaluate the risk of
798 leaching in a sandy loam soil profile. *Pest Management Science* 67:397–407.
799 <https://doi.org/10.1002/ps.2077>
- 800 Pyzola S (2013) Nitrate Reduction Coupled to Iron (II) and Manganese (II) oxidation In An
801 Agricultural Soil. University of Kentucky,
- 802 Reemtsma T, Mehrtens J (1997) Determination of polycyclic aromatic hydrocarbon (PAH) leaching
803 from contaminated soil by a column test with on-line solid phase extraction. *Chemosphere*
804 35:2491–2501. [https://doi.org/10.1016/S0045-6535\(97\)00317-2](https://doi.org/10.1016/S0045-6535(97)00317-2)
- 805 Rennert T, Meißner S, Rinklebe J, Totsche KU (2010) Dissolved Inorganic Contaminants in a
806 Floodplain Soil: Comparison of In Situ Soil Solutions and Laboratory Methods. *Water Air*
807 *Soil Pollut* 209:489–500. <https://doi.org/10.1007/s11270-009-0217-3>
- 808 Rennert T, Rinklebe J (2010) Release of Ni and Zn from Contaminated Floodplain Soils Under
809 Saturated Flow Conditions. *Water Air Soil Pollut* 205:93–105.
810 <https://doi.org/10.1007/s11270-009-0058-0>
- 811 RFSC (2019) R: A language and environment for statistical computing. R Foundation for
812 Statistical Computing
- 813 Roden EE, Wetzel RG (2002) Kinetics of microbial Fe (III) oxide reduction in freshwater wetland
814 sediments. *Limnology and Oceanography* 47:198–211
- 815 Schlautman MA, Morgan JJ (1993) Effects of aqueous chemistry on the binding of polycyclic
816 aromatic hydrocarbons by dissolved humic materials. *Environ Sci Technol* 27:961–969.
817 <https://doi.org/10.1021/es00042a020>

- 818 Schuwirth N, Hofmann T (2006) Comparability of and Alternatives to Leaching Tests for the
819 Assessment of the Emission of Inorganic Soil Contamination (11 pp). *J Soils Sediments*
820 6:102–112. <https://doi.org/10.1065/jss2005.10.149>
- 821 Seidl M, Gromaire M-C, Saad M, De Gouvello B (2013) Effect of substrate depth and rain-event
822 history on the pollutant abatement of green roofs. *Environmental Pollution* 183:195–203.
823 <https://doi.org/10.1016/j.envpol.2013.05.026>
- 824 Seidl M, Huang V, Mouchel JM (1998) Toxicity of combined sewer overflows on river
825 phytoplankton: the role of heavy metals. *Environmental Pollution* 101:107–116.
826 [https://doi.org/10.1016/S0269-7491\(98\)00008-6](https://doi.org/10.1016/S0269-7491(98)00008-6)
- 827 Shaheen SM, Rinklebe J (2014) Geochemical fractions of chromium, copper, and zinc and their
828 vertical distribution in floodplain soil profiles along the Central Elbe River, Germany.
829 *Geoderma* 228–229:142–159. <https://doi.org/10.1016/j.geoderma.2013.10.012>
- 830 Souvestre Q (2013) Aménagement dans une zone de fortes contraintes
- 831 Suna Erses A, Onay TT (2003) In situ heavy metal attenuation in landfills under methanogenic
832 conditions. *Journal of Hazardous Materials* 99:159–175. [https://doi.org/10.1016/S0304-](https://doi.org/10.1016/S0304-3894(02)00354-0)
833 [3894\(02\)00354-0](https://doi.org/10.1016/S0304-3894(02)00354-0)
- 834 Thums CR, Farago ME, Thornton I (2008) Bioavailability of trace metals in brownfield soils in an
835 urban area in the UK. *Environ Geochem Health* 30:549–563. [https://doi.org/10.1007/s10653-](https://doi.org/10.1007/s10653-008-9185-6)
836 [008-9185-6](https://doi.org/10.1007/s10653-008-9185-6)
- 837 Tian W, Wang L, Li D, Li F (2015) Leachability of phenanthrene from soil under acid rain and its
838 relationship with dissolved organic matter. *Environ Earth Sci* 73:3675–3681.
839 <https://doi.org/10.1007/s12665-014-3653-3>
- 840 US EPA (2017) Leaching Environmental Assessment Framework (LEAF) How-To Guide
- 841 US EPA O (2015) The SW-846 Compendium. In: US EPA. [https://www.epa.gov/hw-sw846/sw-](https://www.epa.gov/hw-sw846/sw-846-compendium)
842 [846-compendium](https://www.epa.gov/hw-sw846/sw-846-compendium). Accessed 11 Nov 2020
- 843 Van der Sloot HA (1996) Developments in evaluating environmental impact from utilization of bulk
844 inert wastes using laboratory leaching tests and field verification. *Waste Management* 16:65–
845 81
- 846 Walsh CJ, Roy AH, Feminella JW, et al (2005) The urban stream syndrome : current knowledge and
847 the search for a cure
- 848 Wang W, Massey Simonich SL, Xue M, et al (2010) Concentrations, sources and spatial distribution
849 of polycyclic aromatic hydrocarbons in soils from Beijing, Tianjin and surrounding areas,
850 North China. *Environ Pollut* 158:1245–1251. <https://doi.org/10.1016/j.envpol.2010.01.021>
- 851 Zsolnay A, Baigar E, Jimenez M, et al (1999) Differentiating with fluorescence spectroscopy the
852 sources of dissolved organic matter in soils subjected to drying. *Chemosphere* 38:45–50.
853 [https://doi.org/10.1016/S0045-6535\(98\)00166-0](https://doi.org/10.1016/S0045-6535(98)00166-0)

854